Polyglutamic acid-trimethyl chitosan-based intranasal peptide nano-vaccine induces potent immune responses against group A streptococcus

*Reshma J. Nevagi[a], Zeinab G. Khalil[b,c], Waleed M. Hussein[a], Jessica Powell[d], Michael R. Batzloff[d], Robert J. Capon[b], Michael F. Good[d], Mariusz Skwarczynski[a], Istvan Toth[a,b,e]**

[a] School of Chemistry & Molecular Biosciences, The University of Queensland, St Lucia, QLD 4072, Australia

[b] Institute of Molecular Biosciences, The University of Queensland, St Lucia, QLD 4072, Australia.

[c] Diamantina Institute, The University of Queensland, Woolloongabba, QLD 4102, Australia

[d] Institute of Glycomics, Griffith University, Gold Coast, QLD 4215, Australia

[e] School of Pharmacy, The University of Queensland, Woolloongabba, QLD 4102, Australia

***Corresponding author:** Professor Istvan Toth, School of Chemistry and Molecular Biosciences, The University of Queensland, St Lucia, QLD 4072, Australia. Tel.: +61 7 3346 9892, Fax: +61 7 3365 4273, Email: i.toth@uq.edu.au

Keywords: nanoparticles, polyglutamic acid, trimethyl chitosan, group A streptococcus, vaccine

Abstract

Peptide-based vaccines have the potential to overcome the limitations of classical vaccines; however, their use is hampered by a lack of carriers and adjuvants suitable for human use. In this study, an efficient self-adjuvanting peptide vaccine delivery system was developed based on the ionic interactions between cationic trimethyl chitosan (TMC) and a peptide antigen coupled with synthetically defined anionic α-poly-(L-glutamic acid) (PGA). The antigen, possessing a conserved B-cell epitope derived from the group A streptococcus (GAS) pathogen and a universal T-helper epitope, was conjugated to PGA using cycloaddition reaction. The produced anionic conjugate formed nanoparticles (NP-1) through interaction with cationic

TMC. These NP-1 induced higher systemic and mucosal antibody titers compared to antigen adjuvanted with standard mucosal adjuvant cholera toxin B subunit or antigen mixed with TMC. The produced serum antibodies were also opsonic against clinically isolated GAS strains. Further, a reduction in bacterial burden was observed in nasal secretions, pharyngeal surface and nasopharyngeal-associated lymphoid tissue of mice immunized with NP-1 in GAS challenge studies. Thus, conjugation of defined-length anionic polymer to peptide antigen as a means of formulating ionic interaction-based nanoparticles with cationic polymer is a promising strategy for peptide antigen delivery.

Introduction

Vaccination is one of the best strategies to control or fight against infectious diseases [1]. Traditionally, vaccines were made up of killed or live attenuated bacteria. However, over the past few decades, the focus of vaccine development has shifted to subunit vaccines because of their improved safety profile and manufacturing advantages compared to their traditional counterparts [2]. Peptide subunit vaccines are gaining popularity because they utilize a short, defined, synthetic peptide epitope derived from a specific target pathogen to induce well-defined immune responses without causing adverse effects. They can also be easily chemically synthesized in pure state and at large scale [3]. However, these small-sized peptide epitopes are poorly immunogenic on their own. They lack danger signals, which are required for their recognition by the human immune system [4]. Therefore, immuno-adjuvants or delivery systems are always incorporated into peptide vaccines to enhance their immunogenicity [5]. Immuno-adjuvants are usually designed based on pathogen-associated molecular patterns (PAMP) and are either mixed or formulated with the antigen of interest. Recognition of PAMP by receptors present on antigen-presenting cells (APCs) triggers the cascade of immune responses [6]. Delivery systems, such as nanoparticles (NPs) and liposomes, are known to mimic pathogenic features (e.g. size, shape) and enhance immune response by gaining entry

into APCs [7]. NPs built on the conjugation of peptide epitopes and polymers demonstrated very promising properties; however, their lack of biodegradability could present a serious drawback [8]. Chitosan is a biodegradable, muco-adhesive, non-toxic natural polymer that is known to be recognized by mannose receptors, toll-like receptor 2, C-type lectin receptor Dectin-1 and leukotriene B4 receptors present on APCs [9, 10]. Chitosan formulations have been shown to possess self-adjuvanting properties and improve the immunogenicity of peptide-based vaccines [11]. Chitosan NPs are usually prepared by charge-charge interactions with an anionic crosslinker, antigen or polymer [12, 13]. Previous studies on chitosan NPs for subunit vaccine delivery were typically based on the use of anionic tripoly-phosphate (TPP) as a crosslinking agent [14]. Safari et al. formulated chitosan-TPP NPs to incorporate commercial pneumococcal conjugate vaccine and observed that these NPs induced IgG antibodies comparable to those induced by antigen mixed with commercial Quil-A adjuvant [15]. Vivanco-Cid et al. recently mixed two protein antigens, bovine serum albumin or E protein from dengue virus serotype 2, with chitosan-TPP NPs and showed that these induced primary and secondary humoral immune responses comparable to the commercial adjuvant Alum [16]. Tian et al. formulated chitosan-based NPs by ionic interactions with anionic ovalbumin (OVA) protein antigen, co-loaded with CpG adjuvant [17]. The formulated NPs showed an ability to induce both humoral and cellular immunity in mice. Florindo et al. encapsulated or adsorbed *S. equi* M-like protein (SeM) on poly-ε-caprolactone/glycol chitosan and poly(L-lactic acid)/glycol chitosan NPs [18, 19]. After intranasal immunization in mice, these NPs produced a balanced Th1/Th2 immune response. Our group has also previously prepared NPs from anionic dextran, poly(lactic-co-glycolic acid) (PLGA) and alginate coated liposomes incorporating self-adjuvanting lipopeptide group A streptococcus (GAS) vaccine candidates, and further coated these with trimethyl chitosan (TMC) [20, 21]. The coated NPs induced the production of high levels of mucosal and systemic antibodies that were opsonic against GAS

clinical isolates. Thus, chitosan/TMC NPs can be formulated by ionic interactions, either with negatively charged crosslinker, antigen or polymer(s).

Here, we propose a novel self-adjuvanting vaccine delivery system produced by the conjugation of a short length anionic polymer to a peptide antigen in order to form NPs with cationic TMC by ionic interactions. To examine this new concept, we conjugated peptide antigen to a shorter length synthetic anionic α-poly-(L-glutamic acid) (PGA) polymer. The use of synthetically defined PGA to conjugate peptide antigen was expected to offer advantages, such as improved NP formulation without the need for crosslinkers. PGA is water-soluble, biodegradable, nontoxic, non-immunogenic and clinically tested [22]. It contains numerous side chain carboxylic groups available for interaction with cationic TMC.

GAS is a major pathogen that causes health implications ranging from superficial infection to life-threatening rheumatic heart disease. No vaccine is currently available against GAS [23]. Thus, a peptide (J8P) possessing conserved B-cell epitope derived from GAS M-protein (J8, QAEDKVKQSREAKKQVEKALKQLEDKVQ) and universal T-helper epitope (PADRE, AKFVAAWTLKAAA) [24-26] was conjugated to PGA. The GAS peptide antigen coupled with PGA (PGA-J8P) was further formulated with cationic TMC without the use of a crosslinking agent, lipidation or external adjuvants. This novel vaccine delivery system (NP-1) was evaluated *in vivo* to determine its ability to induce humoral immune responses upon intranasal administration. Mice immunized with NP-1 generated J8-specific mucosal and systemic opsonic antibodies and also showed a reduction in bacterial load in a mucosal GAS challenge study.

2. Experimental

2.1 Materials

Protected Fmoc/Boc-amino acids and (1-[bis(dimethylamino)methylene]-1*H*-1,2,3-triazolo[4,5-b]pyridinium 3-oxid hexafluorophosphate) (HATU) were purchased from

Mimotopes (Melbourne, Australia). Rink amide p-methylbenzhydrylamine (MBHA) resin was purchased from Novabiochem (Hohenbrunn, Germany). *p*-MBHA·HCl resin was purchased from Peptides International (Louisville, USA). *N,N'*-dimethylformamide (DMF), dichloromethane (DCM), methanol, trifluoroacetic acid (TFA), piperidine, HPLC-grade acetonitrile and yeast extract were obtained from Merck (Darmstadt, Germany). 4-Pentynoic acid was purchased from Alfa Aesar (MA, USA). Methyl iodide and sodium chloride were obtained from Chem-Supply (Gilman, SA, Australia). Bovine serum albumin, anti-mouse CD16/CD32, PE/CY7-CD11C, BV605-F4/80, BV421-MHC-II, FITC-CD40, PE-CD80 and APC-CD86 were obtained from eBioscience (CA, USA). *N,N'*-diisopropylethylamine (DIPEA), triisopropylsilane (TIS), acetic anhydride, 2-azidoacetic acid, copper wire, *N*-methyl-2-pyrrolidone (NMP), low molecular weight chitosan (50-190 KDa), sodium iodide, erythrocytes lysing buffer, cholera toxin B subunit (CTB), pilocarpine, phosphate buffered saline (PBS), phenylmethylsulfonylfluoride (PMSF), antimouse IgG, IgA conjugated to horseradish peroxidase and O-phenylenediamine dihydrochloride (OPD) substrate were purchased from Sigma-Aldrich (St Louis, USA). Todd-Hewitt broth (THB) was obtained from Oxoid and horse blood was purchased from Serum Australis (NSW, Australia). Phenol-free IMDM Glutamax medium was obtained from Gibco® Life Technologies (CA, USA).

2.2 Methods

2.2.1 Peptide synthesis

Peptide synthesis was performed on a CEM Discover microwave synthesizer with Synergy software. Electrospray ionization mass spectrometry (ESI-MS) was performed on a Shimadzu (Kyoto, Japan) instrument with Labsolutions software. Analytical reverse-phase high performance liquid chromatography (RP-HPLC) was performed on a Shimadzu instrument using a Vydac analytical C18 column (218TP54; 5 µm, 4.6 mm x 250 mm), Solvent A: 0.1% TFA in water and Solvent B: 0.1% TFA in acetonitrile:water (90:10), flow rate: 1 mL/min,

detection: UV absorbance at 214 nm, method: 0% to 100% linear gradient of solvent B over 40 min. Preparative RP-HPLC was performed on a Shimadzu instrument using a Vydac or Altima preparative C18 column (5 µm, 22 mm x 250 mm) or semi-preparative column (5 µm, 10 mm x 250 mm), flow rate: 5–20 mL/min, detection: UV absorbance at 214 nm. ^{1}H Nuclear magnetic resonance (^{1}H NMR) spectra were recorded on a Bruker Avance 300 MHz spectrometer (Bruker Biospin, Germany).

2.2.1.1 Synthesis of peptide antigen functionalized with alkyne moiety (J8P- alkyne)

Peptide antigen was synthesized using Boc-chemistry on *p*-MBHA·HCl resin (substitution ratio: 0.59 mmol/g, 0.20 mmol, 0.34 g) by microwave-assisted solid-phase peptide synthesis (SPPS). Lysine was used as a linker between PADRE and the J8 sequence. The resin was neutralized with DIPEA. Appropriate Boc-protected amino acids (0.84 mmol, 4.2 equiv) were pre-activated using HATU (0.50 M, 0.80 mmol, 4.0 equiv, 1.6 mL) and DIPEA (1.2 mmol, 6.2 equiv, 0.22 mL) 2 min before coupling to the peptide resin. Double coupling was performed for 5 and 10 min at 70ºC, 20 W to ensure complete coupling. After the coupling of the first amino acid, a capping step was performed using acetic anhydride:DIPEA:DMF (0.5:0.5:9). Boc deprotection (1 min) was performed twice using neat TFA. 4-Pentynoic acid was coupled to the N-terminus of the peptide. Peptide cleavage from the resin was carried out by treatment with hydrofluoric acid (HF) in the presence of *p*-cresol. The crude cleaved peptide was washed with cold ether, filtered, dissolved in acetonitrile:water (50:50) and lyophilized. The obtained peptide was purified by preparative HPLC equipped with a C18 column using a gradient of 30% to 50% of solvent B for 20 min at the flow rate of 20 mL/min. HPLC (C18 column): *t*R = 25.2 min, purity > 98%. MW = 4819.64 g/mol. ESI-MS: *m/z* $[M+3H]^{3+}$= 1607.7 (calc 1607.5), $[M+4H]^{4+}$ = 1206.1 (calc 1205.9), $[M+5H]^{5+}$ = 964.9 (calc 964.9), $[M+6H]^{6+}$ = 804.2 (calc 804.2), $[M+7H]^{7+}$ = 689.5 (calc 689.5), $[M+8H]^{8+}$ = 603.5 (calc 603.4) (see Supporting Information Figures S3 and S4); yield: 15%.

2.2.1.2 Synthesis of α-polyglutamic acid functionalized with azide moiety (PGA-azide):

PGA containing ten glutamic acid residues was synthesized by Fmoc-chemistry on rink amide MBHA resin (substitution ratio: 0.79 mmol/g, 0.20 mmol, 0.25 g) by microwave-assisted SPPS. Fmoc deprotection was performed with 20% piperidine. Fmoc-Glu(OtBu)-OH (0.84 mmol, 4.2 eq, 0.36 g) was activated with HATU (0.50 M, 0.80 mmol, 4.0 eq, 1.6 mL) and DIPEA (1.2 mmol, 5.2 eq, 0.18 mL). Double coupling was performed for 5 and 10 min at 70ºC, 20 W to ensure complete coupling. 2-Azidoacetic acid was coupled at the N-terminus of PGA. PGA-azide was cleaved from the resin using a cocktail of TFA:TIS:water (95:2.5:2.5). The obtained PGA-azide was purified by preparative HPLC using a C18 column with a gradient of 10% to 50% of solvent B for 20 min at a flow rate of 20 mL/min. HPLC (C18 column): *t*R = 12.8 min, purity > 95%. MW = 1391.23 g/mol. ESI-MS: *m/z* $[M+H]^+$ = 1391.7 (calc 1392.2), $[M+2H]^{2+}$ = 696.5 (calc 696.6) (see Supporting Information Figures S5 and S6); yield: 15%.

2.2.2 Synthesis of polyglutamic acid-peptide conjugate (PGA-J8P)

Polyglutamic acid-peptide conjugate (PGA-J8P**)** was synthesized by copper-catalyzed alkyne-azide cycloaddition (CuAAC) reaction [27]. Briefly, a mixture of PGA-azide (9.3 mmol, 2.0 eq, 1.3 mg) and J8P-alkyne (4.3 mmol, 1.0 eq, 2.4 mg) was dissolved in 100 µL of DMF. Copper wires (60-80 mg) pre-treated with concentrated sulphuric acid for 3 min, washed with distilled water and methanol and dried under reduced pressure, were added to the reaction mixture. Initially, the air in the reaction mixture was replaced by bubbling nitrogen (15 sec). The reaction mixture was protected from light by wrapping the flask with aluminum foil. The reaction mixture was stirred at 50°C under nitrogen atmosphere. During the reaction, samples (10 µL) were taken hourly and diluted with 60 µL of solvent B. The progress of the reaction was monitored by ESI-MS and analytical HPLC analysis (see Supporting Information Figure S7). The reaction was completed after 2 h. The blue-to-green-colored reaction mixture was diluted with solvent B and purified by preparative HPLC equipped with a C18 column using a

gradient of 30% to 90% of solvent B for 30 min at a flow rate of 5 mL/min. HPLC (C18 column): *t*R = 24.8 min. MW= 6210.87 g/mol. ESI-MS: m/z $[M+5H]^{5+}$ = 1243.6 (calc 1243.1), $[M+6H]^{6+}$ = 1036.1 (calc 1036.1), $[M+7H]^{7+}$ = 888.2 (calc 888.2), $[M+8H]^{8+}$=777.3 (calc 777.3), $[M+9H]^{9+}$ = 692.2 (calc 691.0) (see Supporting Information Figures S8 and S9); yield: 42%.

2.2.3 Synthesis of *N*-trimethyl chitosan (TMC)

TMC was prepared following a previously reported method [28, 29]. Further information on the synthesis can be found in the supplementary information.

2.2.4 Preparation of NP-1

A solution of PGA-J8P (0.6 mg/mL) was prepared in endotoxin free water. TMC (2 mg/mL) was added drop-wise to the PGA-J8P aqueous solution over 30 min with stirring at room temperature to form NP-1. The PGA-J8P aqueous solution was titrated with different weight ratios of TMC. Surface coating with TMC was verified by monitoring the size and polydispersity index (PDI) of NP-1 during the coating process (Figure 2).

2.2.5 Characterization of NP-1 (particle size, ζ-potential and morphology)

The size and ζ-potential of NP-1 were measured in endotoxin free water by dynamic light scattering (DLS) using a Zetasizer (Nano Series ZS, Malvern Instruments, UK) at 25°C in folded capillary cuvettes. The measurements were taken with a back scattering angle of 173°. The average size of the particles was calculated by the Zetasizer 6.2 software (Malvern Instruments, UK). The morphology of NP-1 was visualized by transmission electron microscopy (TEM; HT7700 Exalens, HITACHI Ltd., Japan) operating at a voltage of 120 kV. The carbon-coated copper grids (Ted Pella, 200 mesh) were glow discharged for 15 sec and 5 µL of sample was mounted. The particles were allowed to deposit on the grid for 2 min. Excess formulation was wicked off with Whatman filter paper and particles were stained with 2% phosphotungstic acid for 30 sec. Excess staining solution was wicked off with Whatman filter

paper, and the grids were air-dried for 5 min in clean conditions before being loaded onto the microscope for viewing.

2.2.6 *In vitro* DCs and macrophages maturation study

Spleens from C57/BL6 mice were passed through a 70 µm cell strainer to obtain single cell suspension of splenocytes in cold complete media (phenol-free IMDM Glutamax medium supplemented with streptomycin (100 µg/mL), penicillin (100 IU/mL), 2-mercaptoethanol (50 µM) and 10% fetal bovine serum). Red blood cells lysis was performed by the addition of 1 mL of erythrocyte lysing buffer followed by incubation on ice for 7 min. Cells were introduced into a 96-well plate at a density of 1×10^6 cells/well and incubated at 37°C for 2 h. NP-1, PGA-J8P, J8P/CTB and J8P/TMC mixtures were added to each well in 25 µM concentration and incubated at 37°C overnight. Cells adhering to the plates were scraped and centrifuged at 350 g for 5 min. The supernatant was discarded, and the cells were incubated for 10 min at 4°C with 50 µL anti-mouse CD16/CD32 diluted (1:1000 v/v) in FACS buffer (1xPBS, 0.02% sodium azide, 0.5% bovine serum albumin). The plates were centrifuged at 350 g for 5 min, the supernatant was discarded and the cells were incubated with 50 µL of antibody cocktail (PE/CY7-CD11C, BV605-F4/80, BV421-MHC-II, FITC-CD40, PE-CD80 and APC-CD86) for 30 min at 4°C in the dark. Cells were then washed three times with increasing amounts of FACS buffer (100 µL, 150 µL and 200 µL). Fixation buffer (50 µL) was added into each well and the cells were incubated for 20 min at room temperature. The wells were then topped up with 150 µL FACS buffer and centrifuged at 400 g for 5 min. The supernatant was discarded and the contents were diluted with 300 µL FACS buffer in a polystyrene flow cytometry sterile test tube. The cells were kept in dark conditions at 4°C until analyzed using a BD LSRII flow cytometer (BD Biosciences, CA, USA).

2.2.7 *In-vivo* murine study

All animal protocols were approved by the Griffith University Research Ethics Review Board (GU Ref No. GLY-01-15-AEC) in accordance with Australian National Health and Medical Research Council (NHMRC) guidelines. Six-week old female inbred C57/BL6 mice obtained from the Animal Resource Centre (Perth, Western Australia) were divided into five groups of 10 mice each. Negative control mice were intranasally administered with PBS (10 µL/nare), while positive control mice received an intranasal physical mixture of J8P and CTB (10 µg each) in 20 µL of water. Other groups were administered with NP-1 (containing 10 µg of J8P), J8P peptide alone (10 µg) or a physical mixture of J8P/TMC (10 µg of J8P) in 20 µL water (10 µL/nare). All mice were intranasally immunized on day 0, followed by boosts on days 21 and 42.

2.2.8 Sample collection

Serum samples were collected on days 20, 41 and 55 post primary immunization to determine the level of J8-specific IgG antibodies. Blood (10 µL) collected via tail snip was added to PBS (90 µL) and centrifuged at 4000 g for 10 min to collect sera. Clear supernatant was stored at -20ºC for further analysis. Saliva was collected on days 6, 27 and 48 post primary immunization to determine the level of J8-specific IgA antibodies. Mice were given 50 µL of 0.1% pilocarpine intraperitoneally (i.p.) and left for 2 min before collecting saliva. Collected saliva was added to 1 µL of PMSF, a protease inhibitor solution, and stored at -80ºC for further analysis.

2.2.9 Determination of antibody titers

To determine J8-specific IgG and IgA antibody titers, enzyme-linked immunosorbent assays (ELISA) were performed [30]. Flat bottom 96-well plates were coated with J8 peptide (5 µg/well) and blocked with 5% skim milk. Two-fold serial dilutions were performed for serum IgG (1:200) and salivary antibodies (1:4). Horseradish peroxidase conjugated secondary antibody (IgG or IgA) was added to the plate and color development was observed after adding

OPD substrate. Optical density was measured at 450 nm using a microplate reader (Molecular Devices, CA, USA). Antibody titers were determined by the lowest dilution showing an optical density greater than the average + 3 standard deviations (SD) of control wells (sera/saliva from the negative control group). The data were statistically analyzed by one-way ANOVA followed by Tukey post-hoc test.

2.2.10 Intranasal GAS challenge study

Mice were challenged 20 days after the second boost with a dose of 5×10^6 colony-forming unit (CFU)/10 µL streptomycin-resistant M1 GAS strain, which was serially passaged in mouse spleen to enhance virulence [31]. Twenty-four hours prior to intranasal challenge with GAS, streptomycin (200 µg/mL) was included in mouse drinking water. On the day of challenge, mice were anaesthetized with an i.p. injection of 75-100 µL of Ketamine:Xylazine (1:1) dissolved in 10 mL of water, and challenged with the bacterial sample (10 µL/mouse). Mice were laid on their back, nose facing upward, to encourage ingestion of the bacteria. One mouse from the positive control group died prior to bacterial challenge.

2.2.11 Nasal shedding, throat swabs and nasal associated lymphoid tissue

Nares of each mouse were pressed ten times (on days 1 and 2 post-challenge) onto the surface of Columbia blood agar (CBA) plates containing 2% defibrinated horse blood with 200 µg/mL streptomycin. The plates were cultured in duplicate for each mouse. The plates were streaked out and incubated overnight at 37°C. Mouse throats were swabbed using a sterile Minitip Flaq Swab (COPAN Diagnostics, Corona, CA, USA) moistened with sterile PBS on days 1 and 2 post-challenge. The throat swabs were also cultured on CBA plates containing 2% defibrinated horse blood and 200 µg/mL streptomycin and incubated overnight at 37°C. On day 3 post-challenge, mice were culled by CO_2 asphyxiation. Nasal associated lymphoid tissue (NALT) samples were collected in sterile PBS containing 15 mM EDTA and homogenized in a bullet-blender homogenizer. Subsequently, NALT samples were serially diluted from 10^{-1} to 10^{-3} and

20 µL was plated on CBA plates in duplicate using the pour plate method. The plates were incubated overnight at 37°C. All plates were stored at 4ºC until individual hemolytic GAS colonies were counted.

2.2.12 Opsonization assay

The sera of mice collected on 13 days after the second boost were tested in an indirect bactericidal assay to evaluate the opsonic ability of serum IgG antibodies against various GAS strains [21]. The clinical isolates examined in this assay were ACM-5199 (ATCC 12344, NCIB 11841, scarlet fever); ACM-5203 (ATCC 19615, pharynx of child following the episode of sore throat); GC2 203 (wound swab); D3840 (nasopharynx swab); and D2612 (nasopharynx swab). Bacteria were plated on THB plates supplemented with 5% yeast extract and incubated at 37°C for 24 h. A single colony from each bacterium was transferred to 5 mL of THB supplemented with 5% yeast extract and incubated for 24 h at 37°C to obtain approximately 4-5 × 10^6 CFU/mL. Cultures were serially diluted to 10^{-2} in PBS. Aliquots (10 µL) were mixed with 20 µL of heat-inactivated sera and 80 µL of horse blood, and incubated in 96-well plates at 37°C for 3 h. Sera were inactivated by heating in a water bath at 50°C for 30 min. Aliquots (10 µL) from the 96-well plate were then plated on THB plates supplemented with 5% yeast extract containing 5% horse blood. Plates were incubated at 37°C for 24 h and bacterial survival was analyzed by enumerating CFU. Opsonic activity of the antibodies (anti-peptide) sera (% reduction in mean CFU) was calculated as [1-(CFU in the presence of anti-peptide sera)/(mean CFU in the presence of sera from negative control group)] × 100 [32]. The assay was performed in triplicate from three independent cultures.

3. Results

3.1 Synthesis of PGA-J8P and TMC

A copper-catalyzed alkyne-azide 1,3-dipolar cycloaddition “click” reaction was employed to conjugate PGA to the J8P peptide (Figure 1) [27]. Firstly, peptides possessing J8 and PADRE

sequences (J8P) were synthesized by Boc-SPPS. 4-Pentynoic acid was coupled to the N-terminus of the peptide to functionalize it with the alkyne moiety (J8P-alkyne). PGA was synthesized using Fmoc-SPPS and modified with 2-azidoacetic acid on its N-terminus (PGA-azide). The J8P-alkyne and PGA-azide were then conjugated via CuAAC reaction using Cu wires in DMF [28, 29]. Two equivalents of PGA-azide were used to ensure the complete consumption of J8P-alkyne. The reaction was monitored by ESI-MS and HPLC, and was completed in 2-3 h.

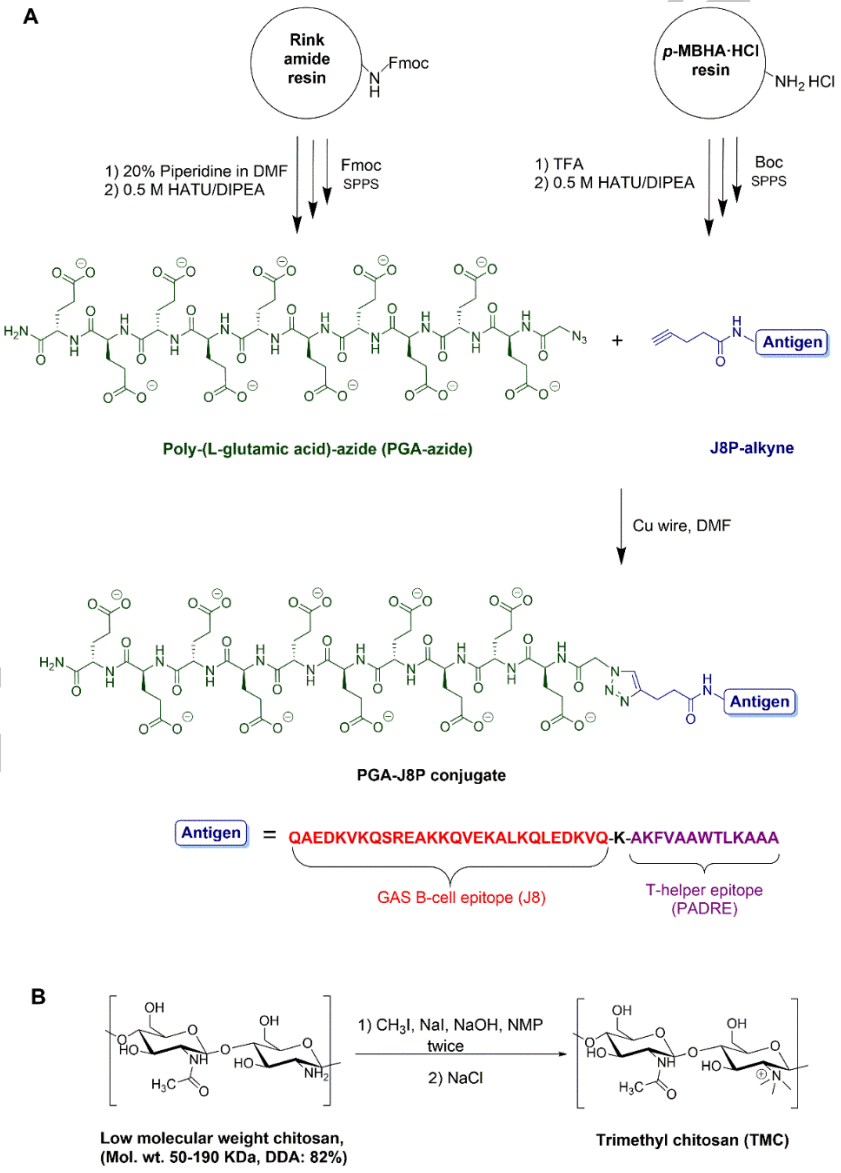

Figure 1. Schematic illustration of the synthetic procedure for PGA-J8P (A) and TMC (B).

TMC was produced by methylation of chitosan using methyl iodide under alkaline conditions by the two-step method [28]. It was observed that the degree of trimethylation was relatively low (<50%) after completion of single methylation. The water solubility of TMC is highly dependent on the degree of methylation; thus, a higher level of trimethylation was desired [33]. When double methylation was performed, 74% of the amine groups of chitosan were substituted with trimethyl groups and 16% with dimethyl groups. The degree of *N*-acetylation was 10%.

3.2 Formulation optimization of NP-1

NP-1 were prepared by the ionic interactions of cationic TMC with anionic PGA-J8P peptide antigen (Figure 2A). Aqueous TMC solution was added dropwise into an aqueous solution of PGA-J8P under magnetic stirring at room temperature, enabling the formation of NPs over a period of time without using high-energy forces. The formation of NP-1 was monitored by DLS (see Supporting Information Table 1 and Figure S11). Figure 2B summarizes the changes in particle size and PDI at different weight ratios of PGA-J8P/TMC.

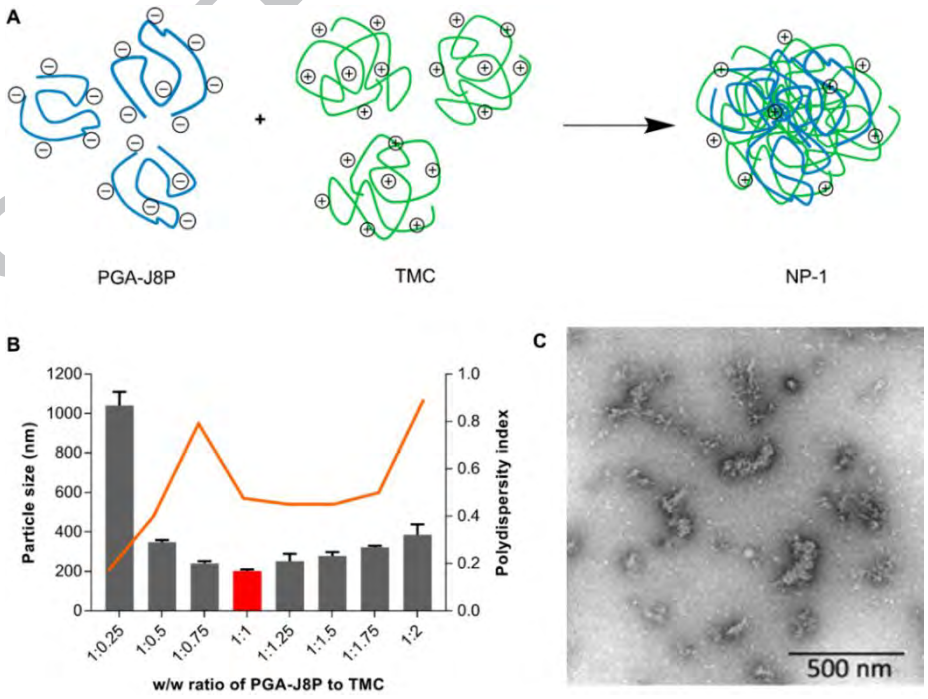

Figure 2. Schematic illustration and characterization of NP-1. (A) Schematic illustration of the preparation of NP-1. (B) Overview of the change in size and PDI of NP-1. Data is represented as mean ± SD. (C) TEM image of NP-1 formed by 1:1 w/w of PGA-J8P to TMC (scale bar = 500 nm).

The NP-1 formed using equal weight ratios of PGA-J8P to TMC (1:1 w/w) possessed the lowest particle size (201 ± 8 nm) with a PDI of 0.33. The further addition of TMC (up to 2 w/w) increased both the particle size and PDI. Hence, NP-1 formed using equal weight ratios of PGA-J8P/TMC were chosen for *in vivo* murine study. These NP-1 were morphologically characterized by TEM (Figure 2C). TEM images of the PGA-J8P/TMC confirmed the formation of NP-1 with similar sizes to those detected by DLS (see Supporting Information Figures S12 and S13).

3.3 *In vitro* DCs and macrophages maturation study

The ability of NP-1 to induce the maturation of dendritic cells (DCs) and macrophages was evaluated *in vitro* using murine splenic CD11c+ dendritic cells and F4/80+ macrophages. Splenic cells were cultured with negative control PBS, positive control J8P/CTB mixture, NP-1, PGA-J8P alone and J8P/TMC mixture in triplicate in a concentration of 25 μM peptide. The expression of maturation markers was measured by flow cytometry. NP-1 and the J8P/CTB mixture were more effective in stimulating MHC-II and CD80 in both DCs and macrophages, compared to negative control (Figure 3). NP-1 induced higher expression of MHC-II in DCs and macrophages, compared to soluble PGA-J8P and J8P/TMC mixture ($p < 0.001$).

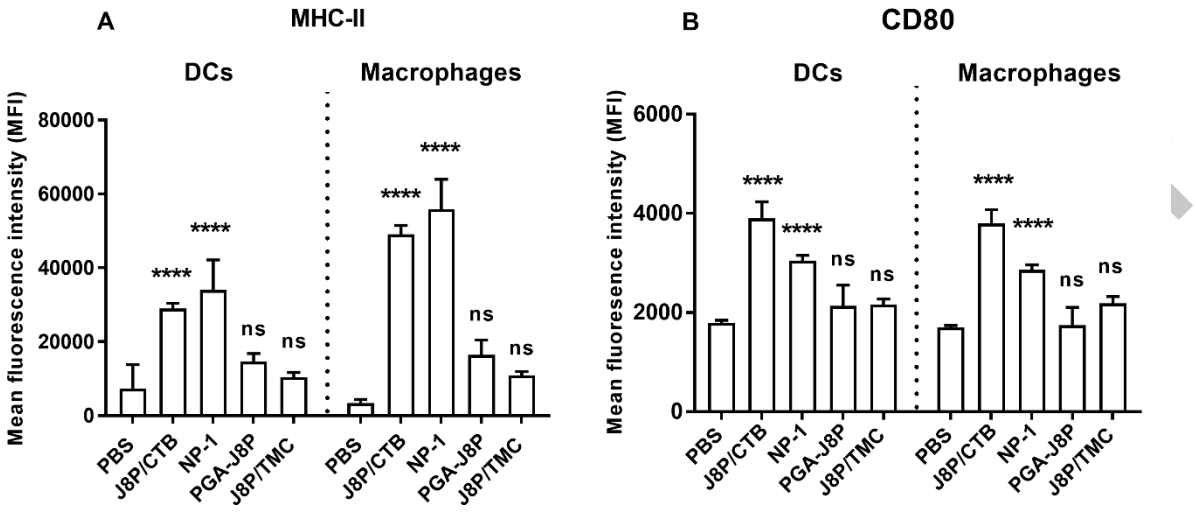

Figure 3. Expression of MHC-II and CD80 on the surface of CD11c+ DCs and F4/80+ macrophages as analyzed by flow cytometry (n = 3). (**A**) Mean fluorescence intensity of isolated CD11c+ dendritic cells and F4/80+ macrophages for MHC-II expression. (**B**) Mean fluorescence intensity of isolated CD11c+ dendritic cells and F4/80+ macrophages for CD80 expression. Data is represented as mean ± SD. Statistical analysis was performed using two-way ANOVA followed by Tukey's multiple comparison test. Not significant (ns), $p > 0.05$; *, $p < 0.05$; **, $p < 0.01$; ***, $p < 0.001$; ****, $p < 0.0001$.

3.4 Immunogenicity of NP-1

Ten mice in each group were intranasally administered with NP-1, PGA-J8P alone or physical mixtures of J8P with TMC. Negative control mice received PBS, whereas positive control mice received a physical mixture of J8P with commercial mucosal adjuvant CTB. All groups received the same concentrations of J8P (10 µg/mouse) in 20 µL water. The serum IgG and salivary IgA antibody titers obtained on day 55 post-primary immunization are shown in Figure 4. It was observed that NP-1 induced higher levels of J8-specific serum IgG and salivary IgA compared to PBS and other groups. When a low dose of J8-based antigen (10 µg/mouse) mixed with commercial adjuvant CTB was administered to mice, the IgA antibody titers were significantly lower compared to those produced by mice immunized with the same amount of the antigen in the form of NP-1. Additionally, mice administered with PGA-J8P alone or

J8P/TMC physical mixture showed significantly lower IgG and IgA titers than mice that received NP-1.

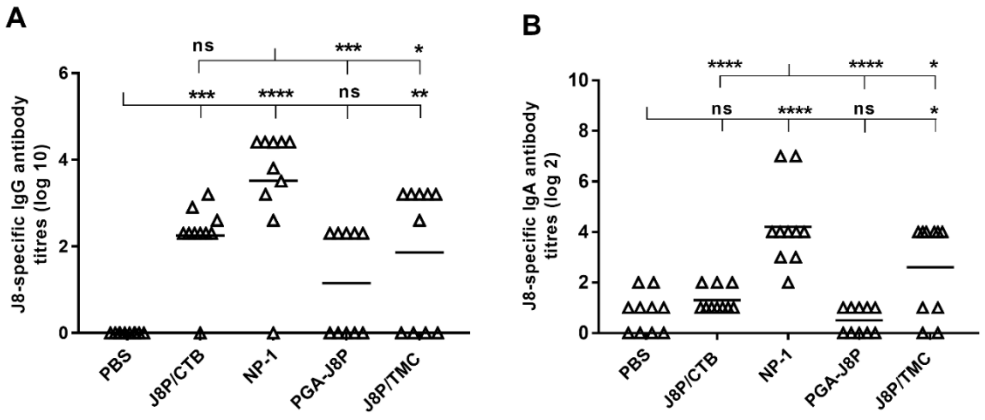

Figure 4. J8-specific antibody responses post-intranasal administration of vaccine NP-1 and controls in C57/BL6 mice (n=10), as determined by ELISA. (A) J8-specific serum IgG titers. (B) J8-specific salivary IgA titers. Statistical analysis was performed by one-way ANOVA followed by Tukey's multiple comparisons test to compare test groups against PBS or NP-1, as indicated. Not significant (ns), $p > 0.05$; *, $p < 0.05$; **, $p < 0.01$; ***, $p < 0.001$; ****, $p < 0.0001$). GraphPad Prism version 7.03 was used to perform statistical analyses.

3.5 Protection against GAS infection

To determine protection against GAS, mice immunized with PBS, J8P/CTB mixture, NP-1, PGA-J8P and J8P/TMC mixture were intranasally challenged with the M1 GAS strain. The challenge study clearly demonstrated the capacity of the developed nanoparticulate system (NP-1) to trigger protection against GAS infection. Post-challenge, the bacterial load in nasal discharge was significantly lower on day 2 in mice immunized with NP-1 compared to mice that had received PBS (Figure 5A). Mice that received NP-1 also showed reduced bacterial load in NALT, as well as on the pharyngeal surface (throat swabs) (Figure 5B and C). Physical mixtures J8P/CTB and J8P/TMC, and soluble PGA-J8P failed to protect mice against the M1 GAS strain.

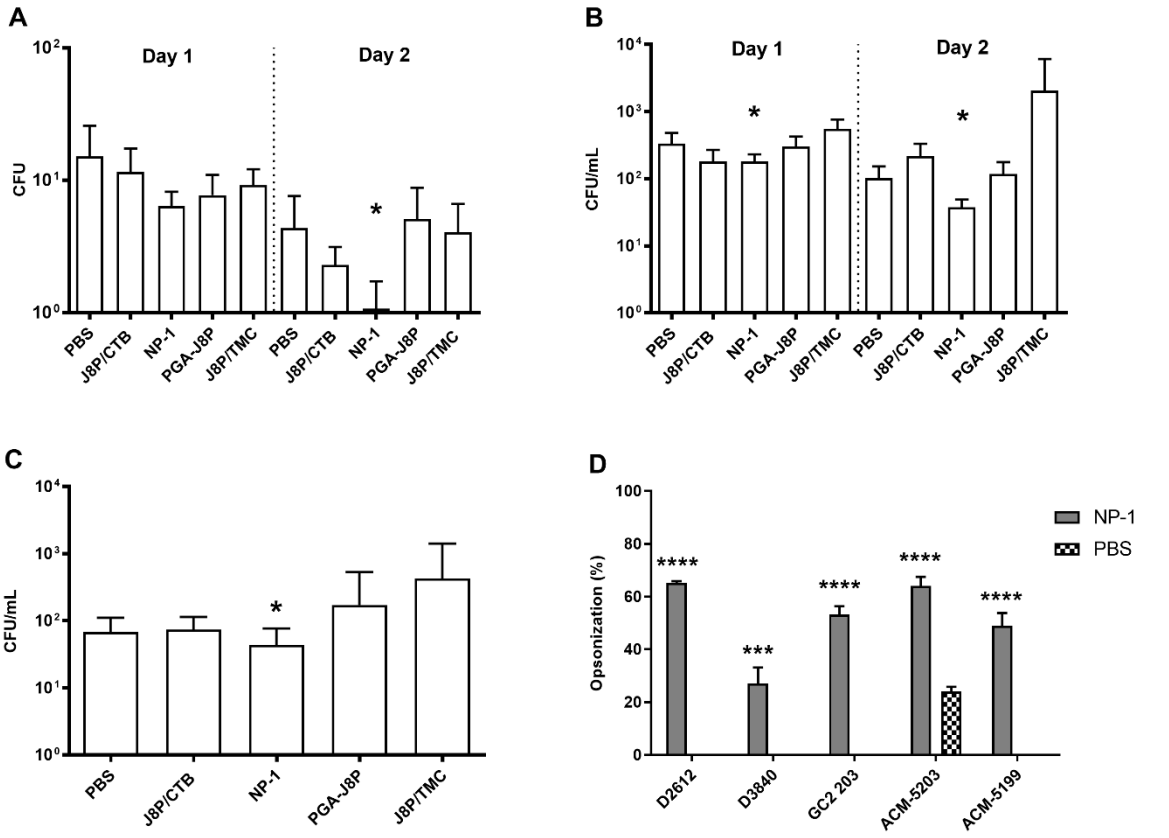

Figure 5. Bacterial burden in nasal shedding (A), throat swabs (B) and NALT (C) following intranasal challenge with the M1 GAS strain in C57/BL6 mice (n = 10/group). The results are represented as the mean CFU + standard error of the mean (SEM). Statistical analyses for throat swabs were performed by repeated measures (RM) two-way ANOVA followed by Tukey's multiple comparisons test, whereas statistical analyses for nasal shedding and NALT were performed by ordinary two-way ANOVA followed by Tukey's multiple comparisons test to compare test groups against PBS. (D) Opsonization of various GAS strains by serum antibodies produced in mice administered with NP-1 and PBS. The average percentage of opsonization for each group is shown with SEM bars. Statistical analyses were performed using two-way ANOVA followed by Sidak's multiple comparisons test to compare against the PBS group. Not significant (ns), $p > 0.05$; *, $p < 0.05$; **, $p < 0.01$; ***, $p < 0.001$, ****, $p < 0.0001$). GraphPad Prism version 7.03 was used to perform statistical analyses.

3.6 Induction of opsonic antibodies against various GAS strains

To determine whether the serum antibodies from mice immunized with NP-1 also possess opsonization activity against other GAS strains, an *in vitro* bactericidal assay was performed against five GAS clinical isolates D2612, D3840, GC2 203, ACM-5203 and ACM-5199. The

J8-specific antibodies produced in the sera of mice immunized with NP-1 showed significant opsonic activity against all tested clinical isolates (Figure 5D).

4. Discussion

The GAS pathogen invades the human body mainly through mucosal surfaces of the upper respiratory tract [23]. Immunization via mucosal routes to prevent colonization and systemic invasion is the preferred approach for the prevention of infections. To develop a mucosal vaccine, we selected chitosan as a delivery platform because of its excellent muco-adhesive properties [34]. Chitosan was reported to be responsible for antigen retention in nasal passages and the opening of tight epithelial junctions, promoting paracellular transport of antigens [9]. The mucosal adhesivity of chitosan is based on ionic interactions between the cationic amine group of the polymer and the negatively charged residues present in mucus [35]. However, chitosan (pKa ~6.5) possesses a positive charge and is water-soluble only at an acidic pH. Therefore, the agglomeration of chitosan formulations at physiological pH is a common problem that dictates the need for water-soluble chitosan derivatives [36]. However, chitosan's trimethylated derivative possesses a permanent cationic charge, is water-soluble over a wide pH range, and demonstrated stronger mucoadhesion, enhanced membrane permeation and absorption at neutral pH [37, 38]. Thus, we methylated the chitosan amine groups with methyl iodide to produce TMC with a high degree of quaternization (74%).

Chitosan/TMC NPs have mostly been formulated by ionic interactions with counter-ions in the form of either crosslinkers, such as TPP, or anionic polymers, such as alginate, dextran or γ-PGA [15-17, 21]. However, crosslinkers may lead to changes in conformation or antigenic properties of the peptide epitope [39], while the use of anionic polymers could lead to an increase in particle size [20]. The formulation of chitosan NPs can be achieved without crosslinkers using the supercritical enhanced atomization spray drying technique [40]. In contrast, we developed a novel simple vaccine delivery strategy by modifying the peptide

antigen itself with defined poly-ions that can further interact with an oppositely charged polymer of interest. To develop cationic NP-1, we conjugated a GAS peptide antigen with short polyanionic PGA via copper-catalyzed alkyne-azide cycloaddition (CuAAC) reaction. Conjugation rendered a negative charge on the peptide antigen, which enabled the formation of NPs with cationic TMC without the use of any external crosslinker. PGA was specifically chosen for conjugation due to its highly anionic nature, similar to polyphosphate crosslinkers. PGA is hydrophilic, fully biodegradable, biocompatible and easy to synthesize in pure state by SPPS [41].

The peptide-PGA conjugate, when mixed with cationic TMC, formed NP-1. It has been shown that NPs 50-200 nm in size are effectively taken up by M-cells and internalized in dendritic cells by receptor-mediated endocytosis [42]. Hence, the mixing of TMC with peptide-PGA conjugate was performed until NP-1 reached 200 nm (measured by DLS). The size of NP-1 was further confirmed with TEM (Figure 2). Surface charge also plays an important role in the presentation of NPs to underlying APCs and the immune stimulation of dendritic cells [43]. It is well-reported that positively charged particles can gain access to APCs, considering electrostatic interaction with negatively charged cell membranes [44]. Thus, NP-1 were formulated in such a manner to achieve a positive ζ-potential value (+36 mV).

Mature APCs play a vital role in the regulation and amplification of immune responses against infectious pathogens [45, 46]. Maturation of DCs and macrophages involves up-regulation of MHC-II expression, which is responsible for antigen presentation to CD4+ T cells and other co-stimulatory molecules, such as CD80 [47]. All tested groups induced expression of MHC-II and CD80 in both DCs and macrophages (Figure 3); however, only positive control (J8P/CTB mixture) and NP-1 induced statistically significant overexpression of these markers compared to PBS ($p < 0.0001$). Interestingly, TMC delivered in simple mixture with antigen (J8P) triggered significantly weaker expression of maturation markers than TMC in the form

of NPs (NP-1). Indeed, TMC in NP form was previously reported to induce higher expression of maturation markers compared to TMC/antigen mixture [48]; likewise, non-formulated chitosan was also found to be a poor or non-inducer of maturation markers [49].

To confirm that NP-1 are able to not only stimulate maturation of APCs, but also trigger antigen specific adaptive immunity, their immunostimulating potential was evaluated through an *in vivo* immunization study. On intranasal administration to mice, NP-1 induced significantly higher serum IgG and mucosal IgA antibody titers against J8 compared to all other tested groups (Figure 4). The physical mixture J8P/CTB produced lower IgA antibody titers compared to NP-1, which indicates superiority of NP-1 over the commercial adjuvant CTB. The presence of TMC in NP-1 was necessary for a strong humoral immune response. Weak IgG and IgA titers were obtained upon the administration of soluble PGA-J8P, indicating an adjuvanting property of TMC. The formation of ionic interaction-based NP-1 was also crucial for the induction of better systemic and mucosal immune responses since the simple physical mixture of J8P with TMC triggered significantly lower IgG and IgA production.

Before systemic invasion into a host, the GAS pathogen readily colonizes mucosal tissues in the nasopharynx and respiratory tract [50]. To determine if NP-1 are effective against bacterial infection through nasopharyngeal mucosal surfaces, a murine challenge model was employed by intranasally administering the M1 GAS strain. A significantly reduced bacterial load was observed from nasal shedding of mice vaccinated with NP-1 compared to PBS-treated mice on day 2 (Figure 5A). The bacterial burden was also significantly reduced in the throats and NALT of mice vaccinated with NP-1 compared to those that received PBS (Figure 5B and 4C). Peptide antigen J8P administered with commercial mucosal adjuvant CTB, soluble PGA-J8P or physical J8P/TMC mixture were ineffective in providing protection to mice against GAS infection. The lack of protection in mice treated with commercial adjuvant can be explained by the relatively poor antibody response triggered by CTB at the tested antigen concentration.

Thus, the ability of antigen formulation (e.g. CTB-based) to trigger maturation of APCs is a necessary but not a sufficient factor for the vaccine efficacy. The effectiveness of a vaccine is also related to the capacity of generated antibodies to opsonize various strains of the bacteria. An indirect bactericidal assay indicated that serum antibodies produced in mice immunized with NP-1 were effective not only against the M1 GAS strain, but also against a variety of clinical isolates (Figure 5D). Overall, NP-1, even at low antigen concentration compared to previous reports [30, 51-53], induced high IgA and opsonic IgG antibody titers and showed protection against GAS infection.

5. Conclusion

The use of synthetically defined PGA greatly enhanced NPs formulation with no external crosslinker. This shows that PGA may not only act as a complexing agent, but potentially also as a crosslinker similar to polyphosphate. Additionally, conjugation of PGA to the peptide antigen rendered negative charge on the antigenic peptide, which allowed formation of NPs with cationic TMC by ionic interaction. This strategy is very effective when a positively charged formulation is desired for neutral or cationic peptide antigens without any anionic polymer coating or additional crosslinker. The developed nanoparticulate peptide vaccine (NP-1) improved the immunogenicity of J8P antigen without any lipidation, suggesting a self-adjuvanting property of this delivery system. Thus, the modification of peptide antigen with PGA followed by the formation of cationic NPs with TMC is a highly promising strategy for peptide antigen delivery.

Supporting information: Mass spectra and HPLC chromatograms for J8P, J8P-alkyne, PGA-azide and PGA-J8P, CuAAC reaction monitoring by HPLC and size measurement of NP-1 by DLS.

Acknowledgements: The authors acknowledge the support of the Australian Microscopy & Microanalysis Research Facility at the Centre for Microscopy and Microanalysis, The

University of Queensland. The authors are thankful to Ms Virginia Nink and Dr Ashwini Kumar Giddam for their help with the flow cytometry experiment.

Funding Sources: This work was supported by the National Health and Medical Research Council [NHMRC Program Grant 1132975]. R. J. Nevagi is supported by a University of Queensland International Scholarship (UQI).

Conflicts of interest: The authors declare no competing interest.

References

[1] S.A. Plotkin, History of vaccine development, Springer Science & Business Media, Philadelphia, 2011.
[2] M. Skwarczynski, I. Toth, Recent advances in peptide-based subunit nanovaccines, Nanomedicine, 9 (2014) 2657-2669.
[3] R.J. Nevagi, I. Toth, M. Skwarczynski, 12 - Peptide-based vaccines A2 - Koutsopoulos, Sotirios, Peptide Applications in Biomedicine, Biotechnology and Bioengineering, Woodhead Publishing2018, pp. 327-358.
[4] M. Skwarczynski, I. Toth, Peptide-based synthetic vaccines, Chemical Science, 7 (2016) 842-854.
[5] C. Foged, T. Rades, Y. Perrie, S. Hook, Subunit vaccine delivery, Springer2015.
[6] S.G. Reed, S. Bertholet, R.N. Coler, M. Friede, New horizons in adjuvants for vaccine development, Trends Immunol., 30 (2009) 23-32.
[7] M.F. Bachmann, G.T. Jennings, Vaccine delivery: a matter of size, geometry, kinetics and molecular patterns, Nature reviews. Immunology, 10 (2010) 787.
[8] M. Skwarczynski, M. Zaman, C.N. Urbani, I. Lin, Z. Jia, M.R. Batzloff, M.F. Good, M.J. Monteiro, I. Toth, Polyacrylate Dendrimer Nanoparticles: A Self- Adjuvanting Vaccine Delivery System, Angew. Chem. Int. Ed., 49 (2010) 5742-5745.
[9] I.M. van der Lubben, J.C. Verhoef, G. Borchard, H.E. Junginger, Chitosan and its derivatives in mucosal drug and vaccine delivery, Eur. J. Pharm. Sci., 14 (2001) 201-207.
[10] W.R. Chen, Chitin, chitosan, and glycated chitosan regulate immune responses: the novel adjuvants for cancer vaccine, Clin. Dev. Immunol., (2013) 1-8.
[11] L. Sáenz, A. Neira-Carrillo, R. Paredes, M. Cortés, S. Bucarey, J.L. Arias, Chitosan formulations improve the immunogenicity of a GnRH-I peptide-based vaccine, Int. J. Pharm., 369 (2009) 64-71.
[12] H. Liu, C. Gao, Preparation and properties of ionically cross- linked chitosan nanoparticles, Polym. Adv. Technol., 20 (2009) 613-619.
[13] A. Rampino, M. Borgogna, P. Blasi, B. Bellich, A. Cesàro, Chitosan nanoparticles: preparation, size evolution and stability, Int. J. Pharm., 455 (2013) 219-228.
[14] C. Prego, P. Paolicelli, B. Díaz, S. Vicente, A. Sánchez, Á. González-Fernández, M.J. Alonso, Chitosan-based nanoparticles for improving immunization against hepatitis B infection, Vaccine, 28 (2010) 2607-2614.
[15] A. Haryono, K. Salsabila, W.K. Restu, S.B. Harmami, D. Safari, Effect of Chitosan and Liposome Nanoparticles as Adjuvant Codelivery on the Immunoglobulin G Subclass Distribution in a Mouse Model, Journal of Immunology Research, 2017 (2017).

[16] I. Izaguirre-Hernández, G. Mellado-Sánchez, K. Mondragón-Vásquez, P. Thomas-Dupont, L. Sánchez-Vargas, K. Hernández-Flores, C. Mendoza-Barrera, V. Altuzar, L. Cedillo-Barrón, H. Vivanco-Cid, Non-Conjugated Chitosan-Based Nanoparticles to Proteic Antigens Elicit Similar Humoral Immune Responses to Those Obtained with Alum, Journal of Nanoscience and Nanotechnology, 17 (2017) 846-852.
[17] Y. Han, Q. Duan, Y. Li, J. Tian, In vitro and in vivo investigation of chitosan–polylysine polymeric nanoparticles for ovalbumin and CpG co-delivery, RSC Advances, 7 (2017) 39962-39969.
[18] H. Florindo, S. Pandit, L. Gonçalves, H. Alpar, A. Almeida, New approach on the development of a mucosal vaccine against strangles: systemic and mucosal immune responses in a mouse model, Vaccine, 27 (2009) 1230-1241.
[19] H. Florindo, S. Pandit, L. Lacerda, L. Gonçalves, H. Alpar, A. Almeida, The enhancement of the immune response against S. equi antigens through the intranasal administration of poly-ε-caprolactone-based nanoparticles, Biomaterials, 30 (2009) 879-891.
[20] N. Marasini, A.K. Giddam, K.A. Ghaffar, M.R. Batzloff, M.F. Good, M. Skwarczynski, I. Toth, Multilayer engineered nanoliposomes as a novel tool for oral delivery of lipopeptide-based vaccines against group A Streptococcus, Nanomedicine (London, U. K.), 11 (2016) 1223-1236.
[21] N. Marasini, A.K. Giddam, Z.G. Khalil, W.M. Hussein, R.J. Capon, M.R. Batzloff, M.F. Good, I. Toth, M. Skwarczynski, Double adjuvanting strategy for peptide-based vaccines: trimethyl chitosan nanoparticles for lipopeptide delivery, Nanomedicine (Lond), 11 (2016) 3223-3235.
[22] A. Ogunleye, A. Bhat, V.U. Irorere, D. Hill, C. Williams, I. Radecka, Poly-γ-glutamic acid: production, properties and applications, Microbiology, 161 (2015) 1-17.
[23] M.W. Cunningham, Pathogenesis of group A streptococcal infections, Clin. Microbiol. Rev., 13 (2000) 470-511.
[24] A. Gedvilaite, I. Kucinskaite-Kodze, R. Lasickiene, A. Timinskas, A. Vaitiekaite, D. Ziogiene, A. Zvirbliene, Evaluation of trichodysplasia spinulosa-associated polyomavirus capsid protein as a new carrier for construction of chimeric virus-like particles harboring foreign epitopes, Viruses, 7 (2015) 4204-4229.
[25] V.P. Kashi, R.A. Jacob, R.A. Shamanna, M. Menon, A. Balasiddaiah, R.K. Varghese, M. Bachu, U. Ranga, The grafting of universal T-helper epitopes enhances immunogenicity of HIV-1 Tat concurrently improving its safety profile, PLoS One, 9 (2014) e114155.
[26] H. Cong, E.J. Mui, W.H. Witola, J. Sidney, J. Alexander, A. Sette, A. Maewal, R. McLeod, Human immunome, bioinformatic analyses using HLA supermotifs and the parasite genome, binding assays, studies of human T cell responses, and immunization of HLA-A* 1101 transgenic mice including novel adjuvants provide a foundation for HLA-A03 restricted CD8+ T cell epitope based, adjuvanted vaccine protective against Toxoplasma gondii, Immunome Res., 6 (2010) 12.
[27] T.-Y. Liu, W.M. Hussein, A.K. Giddam, Z. Jia, J.M. Reiman, M. Zaman, N.A. McMillan, M.F. Good, M.J. Monteiro, I. Toth, Polyacrylate-based delivery system for self-adjuvanting anticancer peptide vaccine, J. Med. Chem., 58 (2014) 888-896.
[28] A. Sieval, M. Thanou, A. Kotze, J. Verhoef, J. Brussee, H. Junginger, Preparation and NMR characterization of highly substitutedN-trimethyl chitosan chloride, Carbohydr. Polym., 36 (1998) 157-165.
[29] V. Mourya, N.N. Inamdar, Trimethyl chitosan and its applications in drug delivery, J. Mater. Sci. Mater. Med., 20 (2009) 1057.
[30] K.A. Ghaffar, N. Marasini, A.K. Giddam, M.R. Batzloff, M.F. Good, M. Skwarczynski, I. Toth, Liposome-based intranasal delivery of lipopeptide vaccine candidates against group A streptococcus, Acta Biomater., 41 (2016) 161-168.

[31] C. Olive, M. Batzloff, A. Horváth, T. Clair, P. Yarwood, I. Toth, M.F. Good, Potential of lipid core peptide technology as a novel self-adjuvanting vaccine delivery system for multiple different synthetic peptide immunogens, Infect. Immun., 71 (2003) 2373-2383.
[32] E.R. Brandt, K. Sriprakash, R.I. Hobb, W.A. Hayman, W. Zeng, M.R. Batzloff, D.C. Jackson, M.F. Good, New multi-determinant strategy for a group A streptococcal vaccine designed for the Australian Aboriginal population, Nat. Med., 6 (2000) 455-459.
[33] R.J. Verheul, M. Amidi, S. van der Wal, E. van Riet, W. Jiskoot, W.E. Hennink, Synthesis, characterization and in vitro biological properties of O-methyl free N, N, N-trimethylated chitosan, Biomaterials, 29 (2008) 3642-3649.
[34] I. Van der Lubben, J. Verhoef, G. Borchard, H. Junginger, Chitosan for mucosal vaccination, Adv. Drug Del. Rev., 52 (2001) 139-144.
[35] L. Illum, I. Jabbal-Gill, M. Hinchcliffe, A. Fisher, S. Davis, Chitosan as a novel nasal delivery system for vaccines, Adv. Drug Del. Rev., 51 (2001) 81-96.
[36] A. Kotze, H. Luessen, A. De Boer, J. Verhoef, H. Junginger, Chitosan for enhanced intestinal permeability: prospects for derivatives soluble in neutral and basic environments, Eur. J. Pharm. Sci., 7 (1999) 145-151.
[37] M. Thanou, J. Verhoef, P. Marbach, H. Junginger, Intestinal absorption of octreotide: N-trimethyl chitosan chloride (TMC) ameliorates the permeability and absorption properties of the somatostatin analogue in vitro and in vivo, J. Pharm. Sci., 89 (2000) 951-957.
[38] J. Hamman, M. Stander, A. Kotze, Effect of the degree of quaternisation of N-trimethyl chitosan chloride on absorption enhancement: in vivo evaluation in rat nasal epithelia, Int. J. Pharm., 232 (2002) 235-242.
[39] F. Zhang, O. Sadovski, G.A. Woolley, Synthesis and Characterization of a Long, Rigid Photoswitchable Cross- Linker for Promoting Peptide and Protein Conformational Change, ChemBioChem, 9 (2008) 2147-2154.
[40] M.A. Rodrigues, L. Figueiredo, L. Padrela, A. Cadete, J. Tiago, H.A. Matos, E.G. de Azevedo, H.F. Florindo, L.M. Gonçalves, A.J. Almeida, Development of a novel mucosal vaccine against strangles by supercritical enhanced atomization spray-drying of Streptococcus equi extracts and evaluation in a mouse model, Eur. J. Pharm. Biopharm., 82 (2012) 392-400.
[41] A. Malhotra, X. Zhang, J. Turkson, S. Santra, Buffer- Stable Chitosan–Polyglutamic Acid Hybrid Nanoparticles for Biomedical Applications, Macromol. Biosci., 13 (2013) 603-613.
[42] N. Csaba, M. Garcia-Fuentes, M.J. Alonso, Nanoparticles for nasal vaccination, Adv. Drug Del. Rev., 61 (2009) 140-157.
[43] Y.J. Kwon, S.M. Standley, S.L. Goh, J.M. Fréchet, Enhanced antigen presentation and immunostimulation of dendritic cells using acid-degradable cationic nanoparticles, J. Controlled Release, 105 (2005) 199-212.
[44] A. Verma, F. Stellacci, Effect of surface properties on nanoparticle–cell interactions, Small, 6 (2010) 12-21.
[45] I. Mellman, R.M. Steinman, Dendritic cells: Specialized and regulated antigen processing machines, Cell, 106 (2001) 255-258.
[46] J. Banchereau, R.M. Steinman, Dendritic cells and the control of immunity, Nature, 392 (1998) 245-252.
[47] J. Banchereau, F. Briere, C. Caux, J. Davoust, S. Lebecque, Y.-J. Liu, B. Pulendran, K. Palucka, Immunobiology of dendritic cells, Annu. Rev. Immunol., 18 (2000) 767-811.
[48] S.M. Bal, B. Slütter, E. van Riet, A.C. Kruithof, Z. Ding, G.F. Kersten, W. Jiskoot, J.A. Bouwstra, Efficient induction of immune responses through intradermal vaccination with N-trimethyl chitosan containing antigen formulations, J. Controlled Release, 142 (2010) 374-383.
[49] K. Brodaczewska, N. Wolaniuk, K. Lewandowska, K. Donskow-Łysoniewska, M. Doligalska, Biodegradable Chitosan Decreases the Immune Response to Trichinella spiralis in Mice, Molecules, 22 (2017) 2008.

[50] S. Brouwer, T.C. Barnett, T. Rivera- Hernandez, M. Rohde, M.J. Walker, Streptococcus pyogenes adhesion and colonization, FEBS Lett., 590 (2016) 3739-3757.
[51] A. Chan, W.M. Hussein, K.A. Ghaffar, N. Marasini, A. Mostafa, S. Eskandari, M.R. Batzloff, M.F. Good, M. Skwarczynski, I. Toth, Structure–activity relationship of lipid core peptide-based group A Streptococcus vaccine candidates, Biorg. Med. Chem., 24 (2016) 3095-3101.
[52] M. Zaman, S. Chandrudu, A.K. Giddam, J. Reiman, M. Skwarczynski, V. McPhun, P.M. Moyle, M.R. Batzloff, M.F. Good, I. Toth, Group A Streptococcal vaccine candidate: contribution of epitope to size, antigen presenting cell interaction and immunogenicity, Nanomedicine, 9 (2014) 2613-2624.
[53] N. Marasini, K. Abdul Ghaffar, A. Kumar Giddam, M. R Batzloff, M. F Good, M. Skwarczynski, I. Toth, Highly immunogenic trimethyl chitosan-based delivery system for intranasal lipopeptide vaccines against group A streptococcus, Curr. Drug Del., 14 (2017) 701-708.

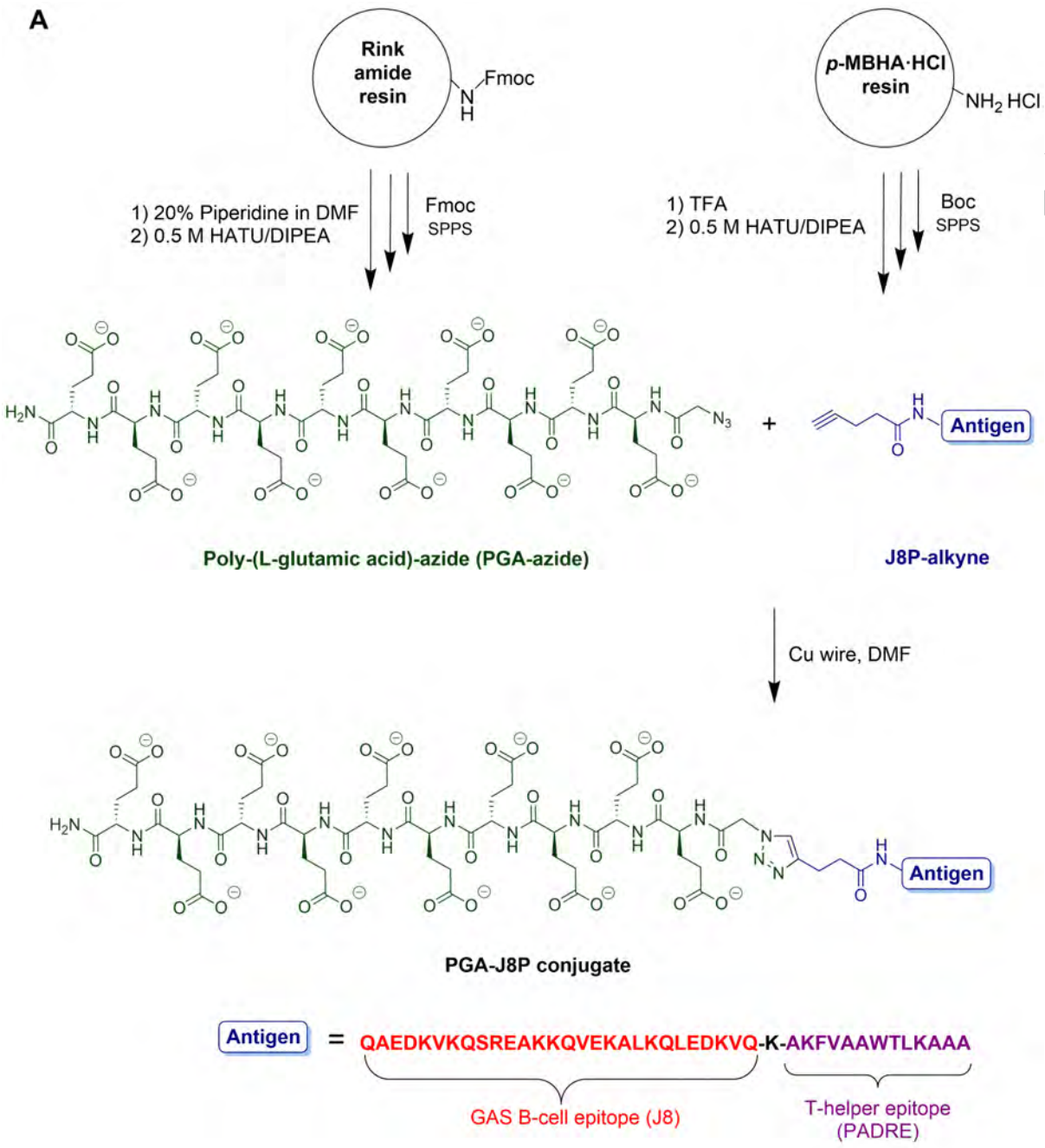
A
Rink amide resin
Fmoc
p-MBHA·HCl resin
NH2 HCl
1) 20% Piperidine in DMF
2) 0.5 M HATU/DIPEA
Fmoc SPPS
1) TFA
2) 0.5 M HATU/DIPEA
Boc SPPS
Antigen
Poly-(L-glutamic acid)-azide (PGA-azide)
J8P-alkyne
Cu wire, DMF
Antigen
PGA-J8P conjugate
Antigen = QAEDKVKQSREAKKQVEKALKQLEDKVQ-K-AKFVAAWTLKAAA
GAS B-cell epitope (J8)
T-helper epitope (PADRE)

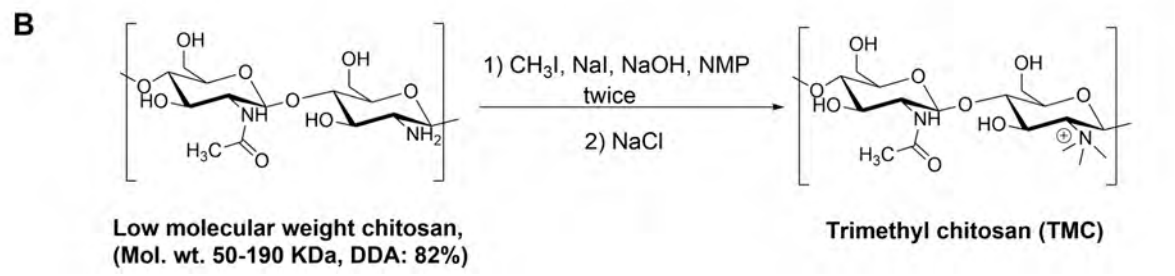
B
1) CH3I, NaI, NaOH, NMP
twice
2) NaCl
Low molecular weight chitosan,
(Mol. wt. 50-190 KDa, DDA: 82%)
Trimethyl chitosan (TMC)

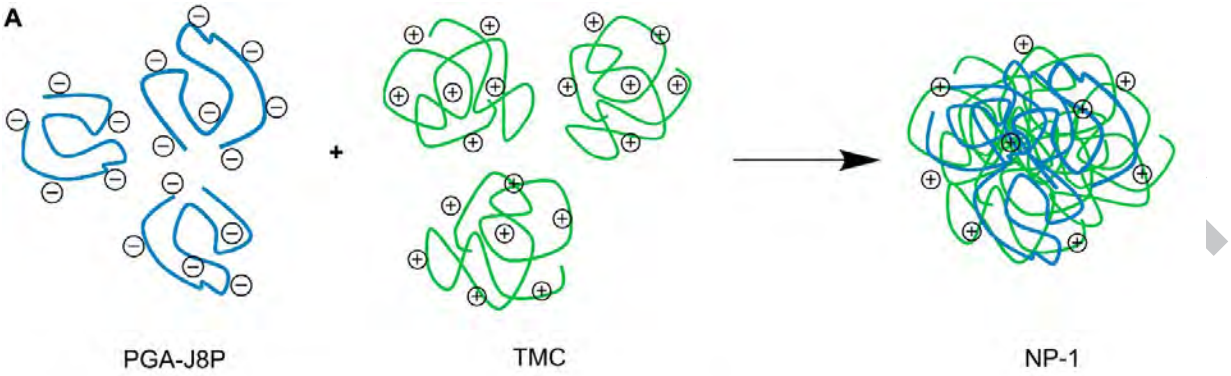
A
PGA-J8P
TMC
NP-1

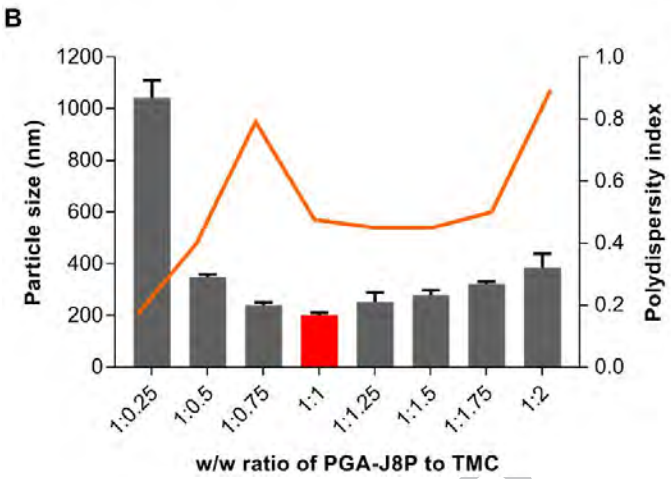
B
Particle size (nm)
Polydispersity index
1200
1000
800
600
400
200
0
1.0
0.8
0.6
0.4
0.2
0.0
1:0.25
1:0.5
1:0.75
1:1
1:1.25
1:1.5
1:1.75
1:2
w/w ratio of PGA-J8P to TMC

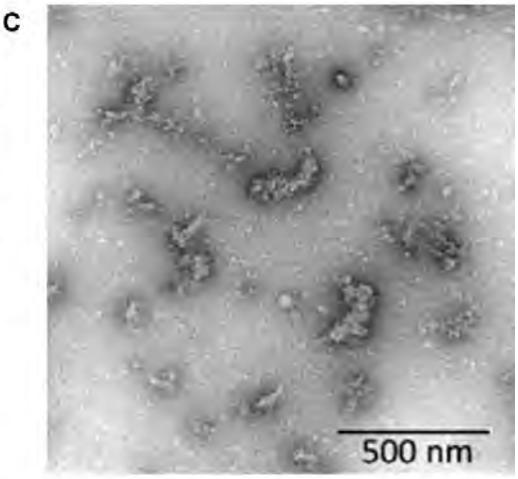
C
500 nm

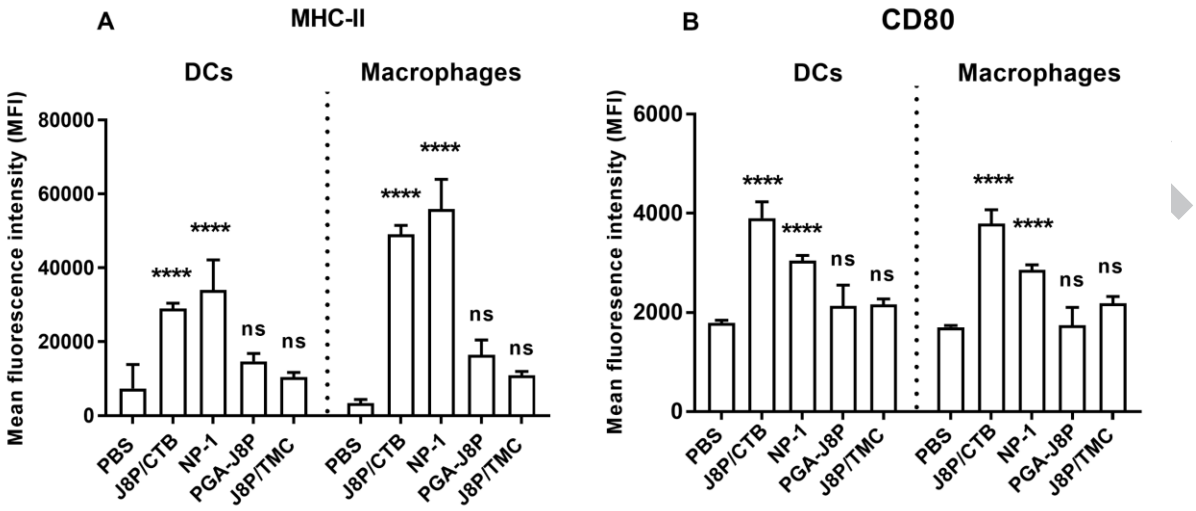

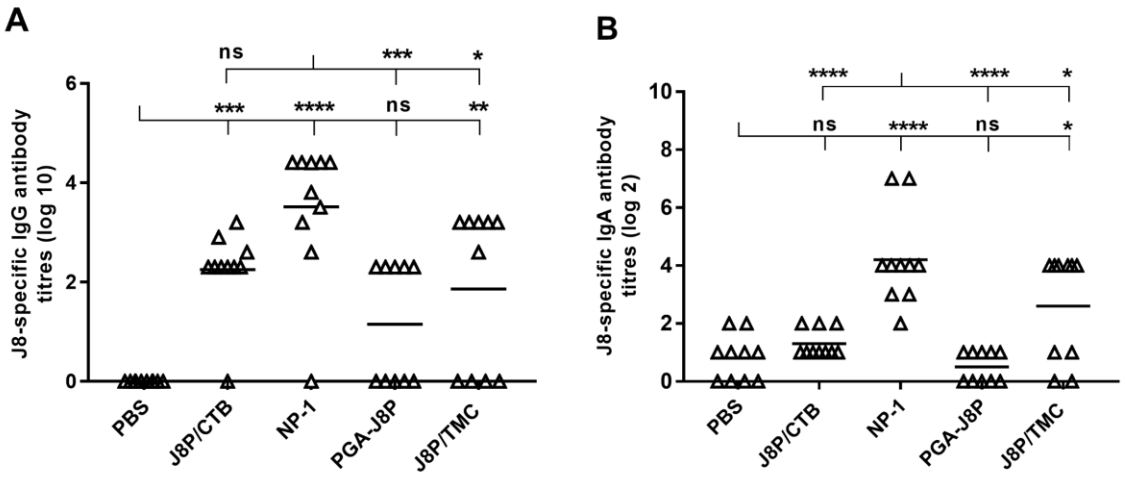

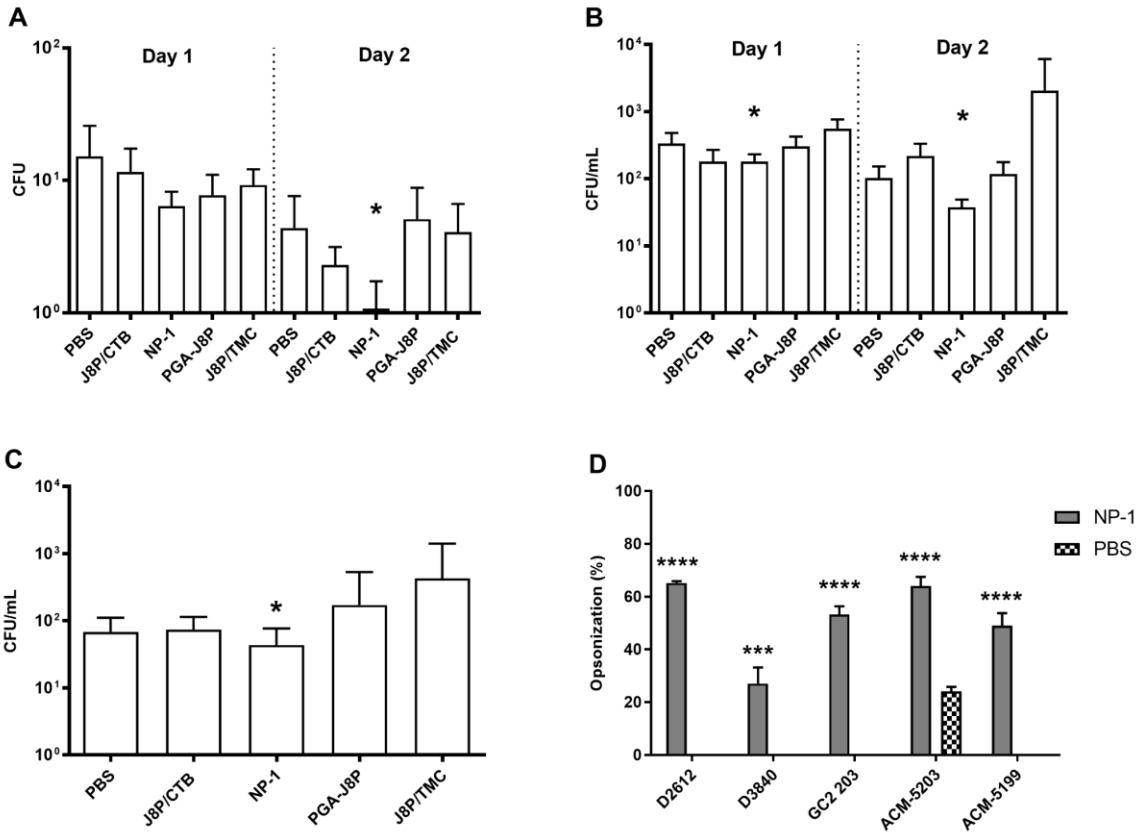

Statement of significance

A self-adjuvanting delivery system is required for peptide vaccines to enhance antigen delivery to immune cells and generate systemic and mucosal immunity. Herein, we developed a novel self-adjuvanting nanoparticulate delivery system for peptide antigens by combining polymer-conjugation and complexation strategies. We conjugated peptide antigen with anionic α-poly-(L-glutamic acid) that in turn, formed nanoparticles with cationic trimethyl chitosan by ionic interactions, without using external crosslinker. On intranasal administration to mice, these nanoparticles induced systemic and mucosal immunity, at low dose. Additionally, nanoparticles provided protection to vaccinated mice against group A streptococcus infection. Thus, this concept should be particularly useful in developing nanoparticles for the delivery of peptide antigens.

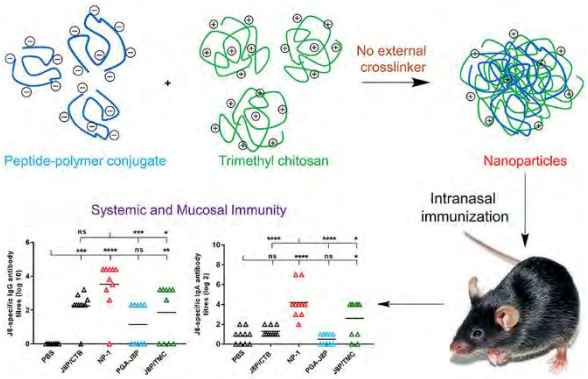

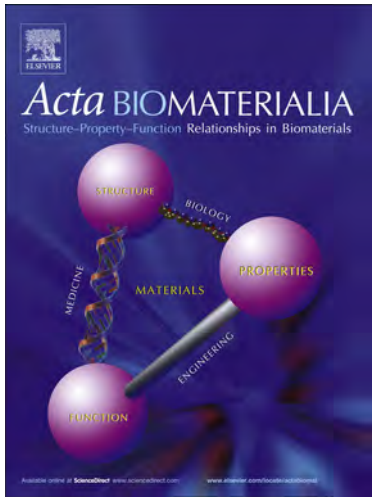

Full length article

Polyglutamic acid-trimethyl chitosan-based intranasal peptide nano-vaccine induces potent immune responses against group A streptococcus

Reshma J. Nevagi, Zeinab G. Khalil, Waleed M. Hussein, Jessica Powell, Michael R. Batzloff, Robert J. Capon, Michael F. Good, Mariusz Skwarczynski, Istvan Toth

PII: S1742-7061(18)30566-X
DOI: https://doi.org/10.1016/j.actbio.2018.09.037
Reference: ACTBIO 5681

To appear in: *Acta Biomaterialia*

Received Date: 11 June 2018
Revised Date: 17 September 2018
Accepted Date: 24 September 2018

Please cite this article as: Nevagi, R.J., Khalil, Z.G., Hussein, W.M., Powell, J., Batzloff, M.R., Capon, R.J., Good, M.F., Skwarczynski, M., Toth, I., Polyglutamic acid-trimethyl chitosan-based intranasal peptide nano-vaccine induces potent immune responses against group A streptococcus, *Acta Biomaterialia* (2018), doi: https://doi.org/10.1016/j.actbio.2018.09.037